J Appl Electrochem (2010) 40:143–149
DOI 10.1007/s10800-009-9990-3

ORIGINAL PAPER

Study of bimetallic corrosion related to Cu interconnects using micropattern corrosion screening method and Tafel plots

Kyle Kai-Hung Yu · Karthikeyan S. M. Pillai · Praveen R. Nalla · Oliver Chyan

Received: 17 March 2009 / Accepted: 16 August 2009 / Published online: 11 September 2009

Abstract On-chip microscopic corrosion, originating from contact of dissimilar metals, can cause serious reliability issues for integrated circuits and microelectromechanical devices. A new micropattern corrosion screening method combined with Tafel plots were employed to study Cu bimetallic corrosion in acid and base solutions relevant to the chemical–mechanical planarization process. The results demonstrated that Cu corrosion on Ru is much more severe compared to Cu corrosion on Ta substrates. Tafel plots confirm the nobility trend of Ru > Cu > Ta. The micropattern corrosion study shows the Cu bimetallic corrosion depends on specific chemicals and bimetallic contacts. Strong complexing ligands like NH_3 combined with energetically favorable Cu/Ru bimetallic contact promote faster Cu corrosion under alkaline conditions ($9 \leq pH \leq 11.4$). Micropattern corrosion screening was shown to be useful in identifying the metastable surface layer during Cu corrosion and determining the optimal benzotriazole concentration for Cu corrosion inhibition.

Keywords Cu corrosion · Bimetallic corrosion · Chemical–mechanical planarization · Corrosion inhibition · Benzotriazole

1 Introduction

In modern microelectronic applications, copper has replaced aluminum as the metal of choice for interconnects because of its higher electrical conductivity [1, 2]. Owing to the lack of volatile byproducts in the reactive ion etching of Cu, the Cu interconnects are fabricated by a damascene patterning process. The process involves etching a trench/through pattern into a dielectric, the blanket deposition of a diffusion barrier followed by Cu electroplating, and finally removal of Cu overburden by chemical–mechanical planarization (CMP) [3–6]. Since the CMP process exposes the Cu interconnect and metal barrier to the continual presence of corrosive chemicals, the resulting bimetallic corrosion can be detrimental to the overall production yields of integrated circuit devices.

The same type of microscopic corrosion that arises during fabrication or in operational use can also be a critical reliability issue for microelectromechanical systems (MEMS) [7, 8]. Previously, we reported a study of microscopic on-chip corrosion of a 17 × 17 μm Digital Light Processing (Texas Instruments) MEMS device [9]. Under optical microscopic examination, the dissimilar metal contact (TiW and Al–Si–Ti) in the MEMS device was identified as the origin of observed corrosion. The accelerated corrosion experiments further reveal that a specific chemical (adsorbed F^- ions) initiated active bimetallic corrosion that was also separately confirmed by galvanic potential measurements. The study suggested that certain energetic bimetallic contacts within the device structures can instigate the onset of catastrophic on-chip corrosion when exposed to appropriate chemical environments. More importantly, the minute dimensions (<μm) involved in a miniature MEMS device can greatly accelerate the corrosion damages that shorten operational lifetime and diminish the device's reliability.

As microelectronic circuits move toward sub 45 nm domains, continued shrinkage of device dimensions makes corrosion-related reliability threats even more acute. In addition, ruthenium (Ru) and other noble metals have been

K. K.-H. Yu · K. S. M. Pillai · P. R. Nalla · O. Chyan (✉)
Department of Chemistry, University of North Texas, Denton, Texas 76203, USA
e-mail: Chyan@unt.edu

actively investigated for use as new diffusion barrier materials for Cu interconnects [10–14]. The increased noble character of diffusion barriers like Ru can further intensify the Cu galvanic corrosion in CMP chemical environments. Therefore, there is a need for an effective methodology to evaluate bimetallic corrosion of Cu interconnects when exposed to CMP and post CMP cleaning conditions.

In this article, we report a novel Micropattern Corrosion Testing technique combined with electrochemistry to allow rapid bimetallic Cu corrosion screening in various chemical environments. Two bimetallic interfaces were investigated using a Cu micro dots pattern ($d = 130$ μm) sputter-deposited on Ta and Ru metal substrates. The Cu/Ta and Cu/Ru micropatterns were immersed in CMP relevant acid and base solutions (H_2SO_4, tartaric, lactic, NH_4OH, and KOH) and their corrosion behaviors were studied in situ under continuous optical microscopic imaging. Corrosion potentials and currents measured by Tafel plots technique complement well with micropattern corrosion testing results to demonstrate an enhanced Cu corrosion in Cu/Ru bimetallic contacts when comparing to Cu/Ta.

2 Experimental

2.1 Micropattern corrosion study

Circular micropatterns of Cu (ca. 50, and 80 nm thick, and 130 μm in diameter) were deposited on selected substrates through a contact mask using a standard DC magnetron sputter (Desktop Pro, Denton Vacuum). Figure 1 depicts the fabrication sequence of the corrosion screening micropattern. The Ru (90 nm) and Ta (180 nm) barrier metal substrates were sputter-deposited on a silicon substrate pre-cleaned by standard organic clean and HF etch [15]. The visual investigation of in situ corrosion processes was carried out using a metallurgical microscope (Nikon, Eclipse ME600) by immersing Cu micropattern structures in testing solutions. This visual inspection approach requires an optical clear solution being used. The solutions of K_2SO_4, tartaric acid, lactic acid, and NH_4OH (0.10 M, Aldrich) were prepared with 18.2 MΩ purified water and pH of the solutions was adjusted from 2 to 11.4 with H_2SO_4 and KOH. After submerging in testing solution, the time-lapsed images of the Cu micropattern were recorded by a computer-controlled digital camera connected to microscope.

2.2 Tafel plots

A potentiostat (CH Instruments, USA) was employed to acquire the open circuit potentials and Tafel plots. Both

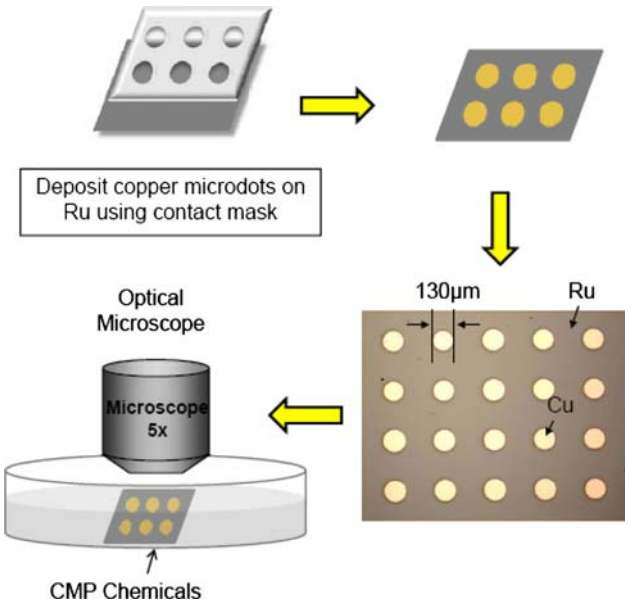

Fig. 1 Fabrication scheme for the Corrosion Screening Micropattern

sputtered Cu, Ta, Ru metal substrates, and solid metal shots were used as electrodes for all electrochemical data. The metal electrodes ($d = 5$ mm) were polished down to 0.5 μm mirror polishing and sonicated in 18.2 MΩ de-ionized water. Three-electrode system with Pt counter and $Hg/HgSO_4$ reference electrodes were employed in a glass cell to obtain Tafel plots data (IV curves) in corresponding solutions used in micropattern corrosion screening. The X-ray photoelectron spectroscopy (XPS) (Phi 5000 VersaProbe, with an Al Kα 58.7 eV excitation source) provided surface chemical composition information.

3 Results and discussion

3.1 Micropattern corrosion study

The specific chemical speciation in the solution has a direct impact on the bimetallic Cu corrosion process. Figure 2 shows the time-lapsed image of Cu micropatterns deposited on Ru substrate (denoted as Cu/Ru) immersed in four different testing solutions at pH = 11.4. The Cu/Ru micropattern screening results indicate that the alkaline NH_4OH induced the fastest Cu corrosion compared with the other three solutions. The time required to completely erode 130 μm Cu microdots can be used as a useful gauge for the relative corrosion trend. Thus, the corrosion rate can be estimated as inversely proportional to the measured corrosion time (t_{corr}) from micropattern corrosion screening. The typical measured corrosion time has ca. 7% error possibly caused by the slight variation of stress and size of sputtered deposited micropatterns. The relative Cu

corrosion rate of Cu/Ru micropattern in four testing solutions follows NH_4OH (33 min) > lactate (113 min) > tartrate (249 min) > KOH/K_2SO_4 (passivated) at pH = 11.4.

The initial oxidation of Cu metal tends to form different oxidized surface films, $Cu_2O/CuO/Cu(OH)_2$ (hydrous oxide) at neutral to high pH [16, 17]. The surface oxide film will act as a barrier between Cu and the corrosive medium to slow further corrosion of underlying Cu. The Cu/Ru micropattern screening confirms the passivation of Cu/Ru microdots immersed in K_2SO_4/KOH of pH 11.4, ref. Fig. 2. Ammonium hydroxide (NH_4OH) is commonly used as a basic buffer and complexing agent in the Cu CMP solution. When exposed to a strong complexing ligand like NH_3, the Cu surface oxide barrier dissolves readily by forming $Cu(NH_3)_2^+$ (formation constant $K_f = 7.24 \times 10^{10}$) and the Cu microdots eroded in 33 min [18]. Accordingly, Cu microdots were found to corrode more slowly in solutions containing lactate and tartrate ions with weaker Cu complexing ability ($K_f \sim 10^{5-6}$) [18].

3.2 Effect of bimetallic contact

In addition to solution environment, the nature of bimetallic contact can also affect the rate of Cu corrosion. Figure 3 shows the time-lapsed images of Cu micropatterns on three different substrates including Ta, Ru, and glass submerged in the alkaline NH_4OH (0.10 M, pH = 11.4). Ta is currently used as part of the liner/diffusion barrier for Cu interconnects in integrated circuit devices [19, 20]. Ru is a new promising liner/barrier metal candidate that allows direct Cu plating to streamline the fabrication process [11, 12]. Glass was chosen as a non-conductive dielectric substrate. As shown in Fig. 3, Cu microdots on Ta substrate require nearly double the amount of time as compared to

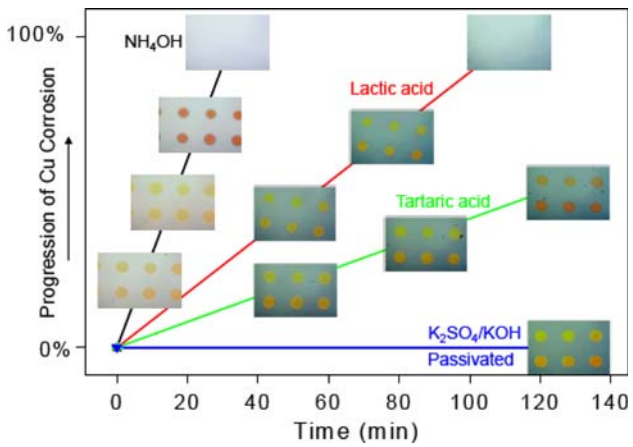

Fig. 2 Time-lapsed optical images of Cu corrosion screening micropatterns submerged in NH_4OH, lactic acid, tartaric acid and K_2SO_4/KOH solutions at pH 11.4. Cu micropatterns were deposited on Ru substrate

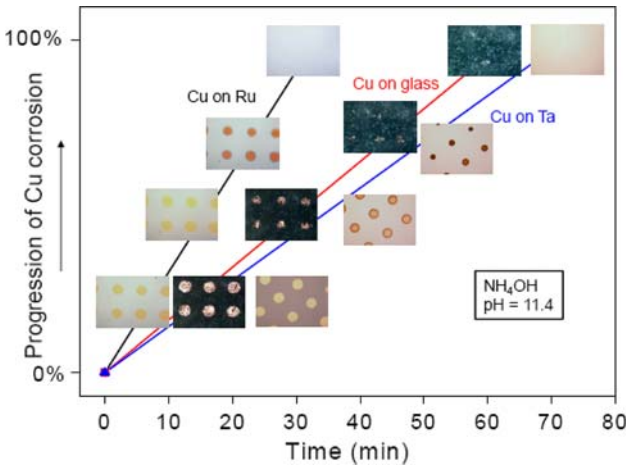

Fig. 3 Time-lapsed optical images of Cu micropatterns deposited on Ru, Ta, and glass substrates, the micropattern corrosion screening was done in NH_4OH solution, pH 11.4

Cu/Ru to corrode completely in NH_4OH pH 11.4 solution. Based on the micropattern screening, the Cu corrosion trend follows Cu/Ru (33 min) > Cu/Glass (63 min) > Cu/Ta (72 min). Similarly, the Cu corrosion rate obtained from Cu/Ru micropattern was found to increase by 4–5 times compared to Cu/Ta in lactate and tartrate pH 11.4 solutions.

Tantalum has a strong tendency to be oxidized and form tantalum oxide (Ta_2O_5) especially when exposed to aqueous medium, Eq. 1.

$$2Ta + 5H_2O = Ta_2O_5 + 10H^+ + 10e^-. \quad (1)$$

The thermodynamically favorable Ta oxidation reaction donates electrons through the Cu/Ta bimetallic contact placing Cu microdots under cathodic protection. In contrast, Ru is nobler than Cu. This inherent nobility of Ru facilitates more Cu oxidation through the galvanic Cu/Ru contact. For all the chemical systems studied in this work, micropattern screening consistently shows enhanced Cu corrosion with Ru contact. It is interesting to note that Cu microdots deposited on a glass substrate, meant to represent a Cu-only corrosion case, exhibits a corrosion rate between Cu/Ru and Cu/Ta as expected, Fig. 3.

3.3 Tafel plots

In order to explore the trend of galvanic corrosion by electrochemistry, Tafel plots were recorded for all four solutions from pH 2 to pH 11.4. Figure 4 depicts typical Tafel plots of Cu, Ta, and Ru metal in NH_4OH pH 9 solution. As shown in Fig. 5, the corrosion potentials mostly follow a general trend of $E_{corr,Ru} > E_{corr,Cu} > E_{corr,Ta}$ which correlates well with the expected metal nobility trend.

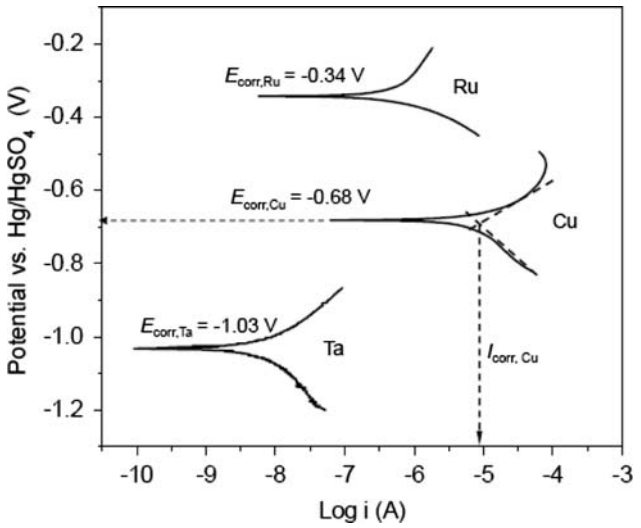

Fig. 4 Tafel plots of Ru, Cu, and Ta measured in NH_4OH solution at pH 9. Corrosion potential (E_{corr}) and corrosion current (I_{corr}) can be obtained from each Tafel plot

Several approaches are commonly employed to provide quantitative measurements of metal corrosion rates [21]. The methods of recording weight-loss and thickness-loss over time are regarded by corrosion engineers to be the "real" corrosion testing. However, this method is a long-term process not suitable for rapid corrosion screening. Tafel plots provide an alternative electrochemical approach that has the advantage of speed and relative simplicity. The rate of corrosion can theoretically be calculated from the corrosion current which obtained from the intersection of two slopes of cathodic and anodic Tafel plots, as illustrated in Fig. 4. The disadvantage is that corrosion rate by Tafel plots is acquired from a fresh electrode/solution and the corrosion studied is limited to the short-term only. Actual corrosion situations are often more complex and with time the metal surface may become partly covered with oxide or other coatings that affect the corrosion rate. Furthermore, Tafel plots based on a single metal electrode cannot be directly applied to study specific bimetallic corrosion that simultaneously involves two overlaying metals.

3.4 Micropattern screening method versus Tafel plots

As demonstrated above, the new micropattern corrosion screening method is better suited for the study of bimetallic corrosion. Different combinations of metals can easily be fabricated into corrosion screening micropatterns, Fig. 1. The micrometer dimension of micropatterns was designed for optical microscope observation. In addition, the thickness of Cu microdots can be adjusted to study a wide dynamic range of corrosion rates within a reasonable experimental time frame, Fig. 6. The micropattern screening not only provides semi-quantitative trend of relative corrosion rate, but also affords a direct visual inspection of actual corrosion processes in real time. The direct imaging of the micropattern is useful in identifying different metastable surface transformations involved in the corrosion process. For instance, Fig. 7 shows that Cu corrosion on Cu/Ru micropatterns can exhibit distinctly different surface transformations in K_2SO_4 as compared to tartaric acid at the same pH = 5. The visual identification serves as an effective pointer to different metastable surface states that await further surface characterization to gain more insight into the corrosion process. Figure 8 shows that the subsequent XPS

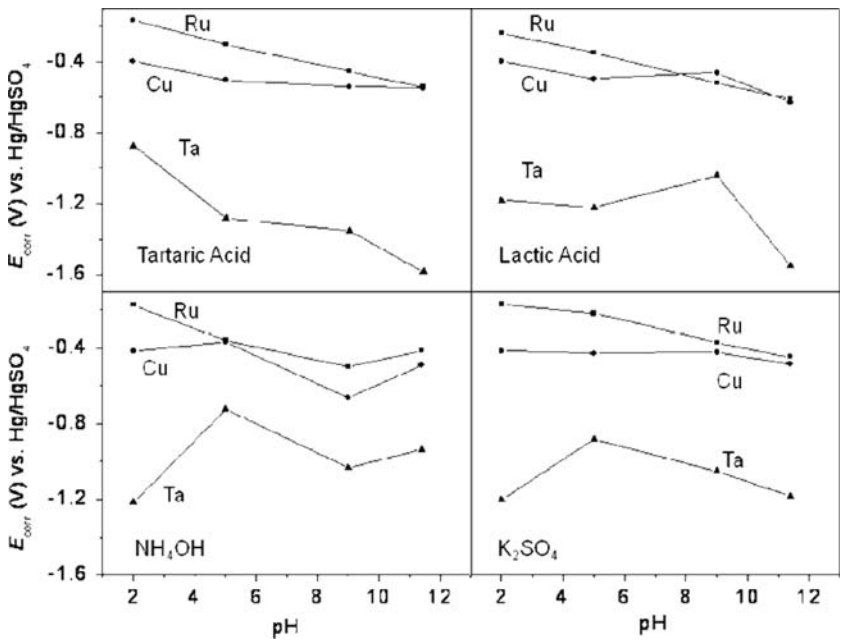

Fig. 5 Corrosion potentials (E_{corr}) obtained from Tafel plots of Ru, Cu, and Ta were plotted versus solution pH

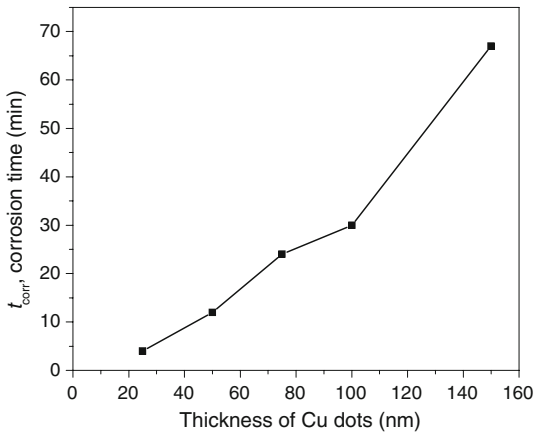

Fig. 6 Corrosion time (t_{corr}) versus the thickness of Cu microdot obtained from Cu/Ru micropattern corrosion screening in NH_4OH solution, pH 11.4

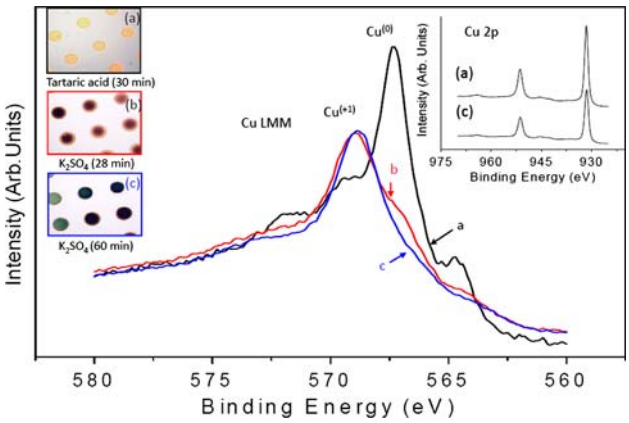

Fig. 8 The Cu LMM auger spectroscopic analyses show Cu surface layers after immersed in K_2SO_4 (pH 5) are mainly Cu^{+1}, but remain Cu^0 in tartaric acid (pH 5). XPS Cu 2p (inset) can't differentiate Cu^{+1} and Cu^0

surface analysis reveals the dark brown/blue coating on Cu microdots after being immersed in K_2SO_4 is mainly Cu(+1) oxide. In comparison, Cu microdots maintain their metallic color and XPS confirms a relatively thin Cu(+1) oxide surface layer on Cu microdots after being immersed in tartaric acid at pH = 5.

In order to compare electrochemical and micropattern approaches, the $I_{corr,Cu}$ obtained from Tafel plots and corresponding t_{corr} from Cu/Ru micropattern screening were plotted in the pH ranging from 2 to 11.4 for three testing solutions. As shown in Fig. 9, both approaches consistently indicate that the Cu corrosion rate decreases when solution pH increases from 2 to 5.

In the acidic region, proton reduction (Eq. 2) will be the main cathodic reaction to sustain the continual Cu oxidation.

$$2H^+ + 2e^- = H_2 \quad (2)$$

Increasing alkalinity slows the proton reduction half reaction and the overall Cu corrosion rate as well. Thus, the observed decreases in $I_{corr,Cu}$ correlate well with increasing t_{corr} obtained from Cu/Ru micropattern screening when the solution alkalinity is raised to pH = 5. It is important to note that separate Cu/Ta micropattern screening experiments reveal all Cu microdots on Ta substrate remain intact even after 10 h of submersion in tartaric acid and K_2SO_4 solutions in all pH tested. The results demonstrated that the new micropattern screening is more capable of detecting the effective cathodic protection of Cu microdots by Cu/Ta bimetallic contact. In comparison, $I_{corr,Cu}$ measured by Tafel plots is based solely on one Cu metal electrode and does not account for the bimetallic factor of Cu/Ru versus Cu/Ta.

For solutions tested in neutral and alkaline conditions (5 < pH ≤ 11.4), Tafel plots (Figure 9a) show a general

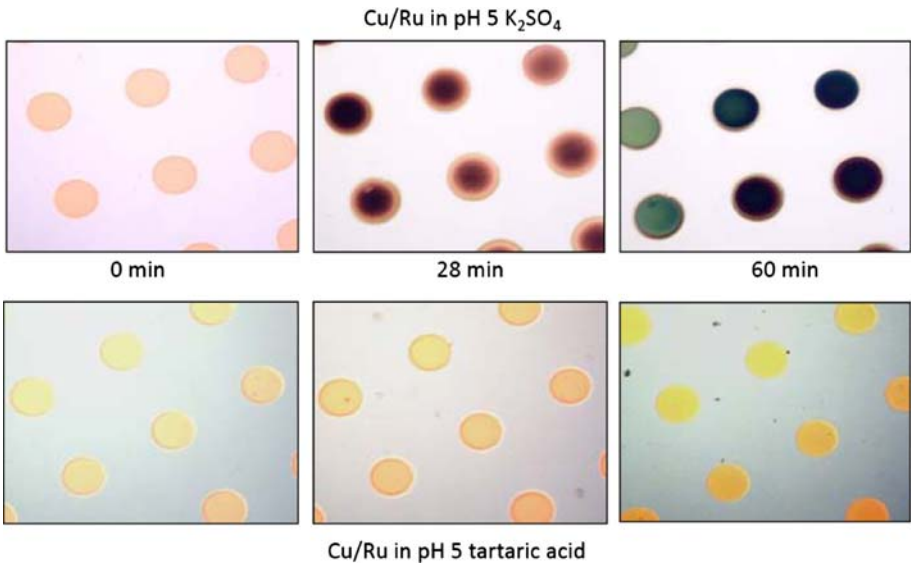

Fig. 7 Micropattern corrosion screening reveals specific chemicals can cause distinctly different surface layers on Cu microdots

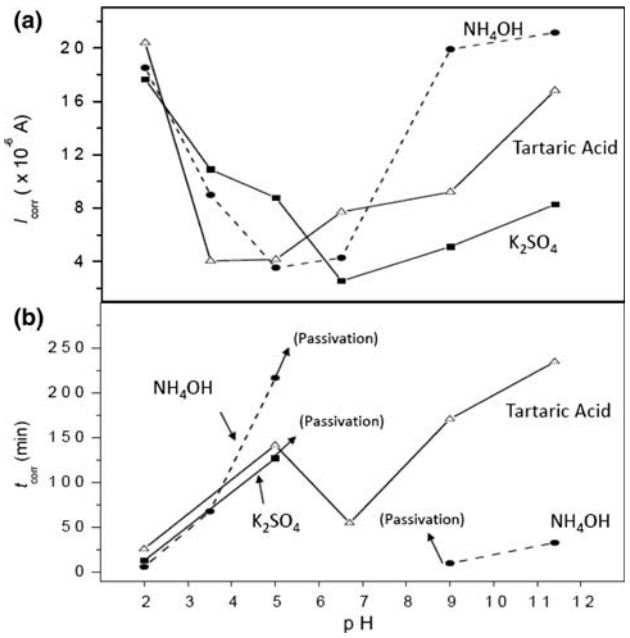

Fig. 9 Corrosion current ($I_{corr,Cu}$) obtained from Cu Tafel plots and corresponding corrosion time (t_{corr}) from Cu/Ru micropattern corrosion screening were plotted in the pH ranging from 2 to 11.4 for NH_4OH, tartaric acid, and K_2SO_4 solutions

trend of a low corrosion current plateau near neutral pH and high corrosion activities at higher pH of 9–11.4. In NH_4OH solution, the Cu/Ru micropattern results (t_{corr}) reflect the similar corrosion trend measured by Cu Tafel plots except the micropattern screening further reveals that a passivation region exists for Cu microdots at the neutral pH, Fig. 9b. In neutral pH aqueous medium, Cu favors the formation of stable surface oxides, mainly Cu_2O. The Cu passivation is easily observable by the Cu/Ru micropattern corrosion study. As the solution alkalinity increases to pH > 9, more NH_3 is available to form soluble complexes with Cu ions and the erosion rate of Cu microdots increased. The micropattern screening results are consistent with the common pH ranges (9–12) utilized in the basic CMP formulation for Cu interconnect [22].

However, the Cu corrosion trend measured by Tafel plots significantly differs from the Cu/Ru micropattern screening result in two other solutions, Fig. 9a, b. For example, in the K_2SO_4 solution of pH > 5, the Cu/Ru micopattern screening indicates Cu microdots were passivated while Tafel plot data show $I_{corr,Cu}$ is varying between 3 and 8 μA/cm^2. For tartaric acid solution of pH > 5, Tafel plot data predict a gradual increase of Cu corrosion rate with solution alkalinity. However, the actual Cu corrosion process observed by Cu/Ru micropattern screening reveals a decreasing Cu corrosion rate with increasing solution pH in tartaric acid solution. The diversion could be the result of dynamic chemical balance between the surface oxide formation (Eq. 3) and oxide dissolution by complex formation (Eq. 4).

$$2Cu + 2OH^- = Cu_2O + H_2O + 2e^- \quad (3)$$

$$Cu_2O + 4\ \text{tartrate}^{2-} + {}^1/_2O_2 + 2H_2O = 2Cu(\text{tartrate})_2^{2-} + 4OH^-. \quad (4)$$

Unlike NH_3, which is a strong Cu complexing ligand, tartrate ions form weaker complexes with Cu ions [$Cu(tartrate)_2^{2-}$ $K_f = 3.23 \times 10^6$] and are less effective in removing the oxidized surface layer from Cu microdots. The Cu/Ru micropattern screening shows that observed t_{corr} increases with increasing alkalinity (6 < pH ≤ 11.4) of tartaric acid solution, Fig. 9b. The trend could be accounted for as the increasing stability of Cu_2O gradually retards the oxide removal process by complex formation with tartrate ions. For the same reason, SO_4^{2-} ions have no complexing ability with Cu ions and Cu microdots were found to be passivated as expected with surface oxides when immersed in K_2SO_4 solutions of pH > 5.

3.5 Cu corrosion inhibitor-benzotriazole

Benzotriazole ($C_6H_5N_3$, BTA) is a Cu corrosion inhibitor most commonly used in Cu CMP solution formulations [23, 24]. During CMP, BTA protects the recessed Cu lines from chemical erosion while the mechanical polishing removes Cu overburden to achieve the overall planarization across the whole wafer. The desirable Cu corrosion inhibition was made possible by a strong chemical reaction of BTA to Cu(+1) surface layer on Cu interconnects [25, 26]. However, it is highly desirable that BTA addition be kept as low as possible because the strongly surface bonded Cu–BTA layer often becomes the source of organic contamination that can affect the conductivity and interlayer adhesion of subsequent Cu interconnects. The micropattern screening method can be used to identify the minimum BTA inhibitor concentration required for a particular chemical environment. For example, Fig. 10 shows the effect of (BTA) concentration on the Cu corrosion time based on Cu/Ru micropattern screening in NH_4OH solution pH = 11.4. With the addition of 2.5 ppm BTA, the Cu corrosion rate of Cu/Ru micropattern was decreased by nearly 10 times. The Cu corrosion rate can be slowed down further over 50 times if 7.5 ppm BTA was added into NH_4OH solution (pH = 11.4). As depicted in the Fig. 10 inset, more BTA (~30 ppm) is needed to achieve the same Cu corrosion inhibition on Cu/Ru micropattern if submerged in a more corrosive NH_4OH solution at pH 10. This example demonstrates how micropattern screening is helpful to identify the minimum threshold concentration of Cu inhibitor BTA needed in specific solution environments and bimetallic contacts.

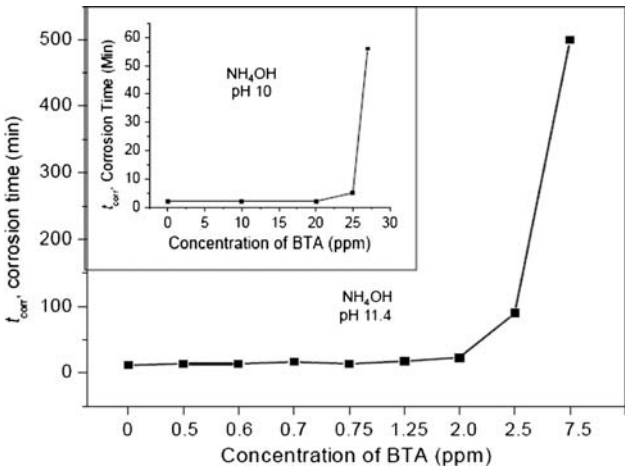

Fig. 10 Effect of corrosion inhibitor, benzotriazole (BTA), on the corrosion time (t_{corr}). Measured by Cu/Ru micropattern in NH_4OH solution, pH 10 and 11.4

In summary, a new micropattern corrosion screen method was demonstrated to be useful in rapid screening bimetallic corrosion in CMP relevant chemical environments. Enhanced Cu corrosion induced by the Cu/Ru bimetallic contact was confirmed with all four solutions studied. The balance between oxide formation and complex reaction can affect the extent of Cu bimetallic corrosion. The alkaline NH_4OH solutions with strong complexing ammonia ligands will result in faster Cu corrosion. For tartaric acid and K_2SO_4 solutions, a slower Cu corrosion process that could lead to Cu passivation was observed based on micropattern screening results. The micropattern corrosion screen method also proves to be useful in identifying the metastable surface states during corrosion and determining threshold BTA concentration for Cu corrosion inhibition.

Acknowledgments The authors acknowledge the Robert A. Welch Foundation (B-1287) and Semiconductor Research Corporation (1292.042) for financial support. Helpful discussion from Trace Hurd, J.D. Luttmer, and Noel Russell toward this study is appreciated.

References

1. Spencer TJ, Osborn T, Kohl PA (2008) Science 320:756
2. Osborn T, He A, Galiba N, Kohl PA (2008) J Electrochem Soc 155:308
3. Banerjee G, Rhoades RL (2008) ECS Trans 13:1
4. Armini S, Whelan CM, Moinpour M, Maex K (2009) J Electrochem Soc 156:18
5. Park JG, Busnaina AA, Hong YK (2008) Microelectronic applications of chemical–mechanical planarization. Wiley, New York, p 467
6. Doi TK (2007) Manuf Eng Mater Process 73:341
7. Melitta H, Frank WD, John TW, Martin K, Carlo C, Roya M (2008) Sens Actuators 145:323
8. Kahn H, Avishai A, Ballarinib R, Heuera AH (2008) Scripta Mater 59:912
9. Chyan O, Chen JJ, Liu M, Chen L, Xu F (1997) J Mater Res 12:3241
10. Kim IK, Cho BG, Park JG, Park JY, Park HS (2009) J Electrochem Soc 156:188
11. Chyan O, Arunagiri TN, Ponnuswamy T (2003) J Electrochem Soc 150:347
12. Chan R, Arunagiri TN, Zhang Y, Chyan O, Wallace RM, Kim MJ, Hurd T (2004) Electrochem Solid State Lett 7:154
13. Lane MW, Murray CE, McFeely FR, Vereecken PM, Rosenberg R (2003) Appl Phys Lett 83:2330
14. Kim IK, Kang YJ, Kwon TY, Cho BG, Park JG, Park JY, Park HS (2008) Electrochem Solid State Lett 11:150
15. Chyan O, JJ Chen, Xu F, Wu J (1997) Anal Chem 69:2434
16. Pourbaix M (1975) Atlas of electrochemical equilibria aqueous solutions. HACE, Houston
17. Gorantla VR, Goia D, Matijevic E, Babu SV (2005) J Electrochem Soc 152:912
18. Dean JA (ed) (1985) Lange's handbook of chemistry, 13th edn. McGraw Hill, New York, p 571
19. Chen CW, Chen JS, Jeng JS (2008) J Electrochem Soc 155:1003
20. Tsao JC, Liu CP, Wang YL, Chen KW (2008) J Nanosci Nanotechnol 8:2582
21. Revie RW (ed) (2000) Uhilig's corrosion handbook, 2nd edn. Wiley-Interscience, New York
22. Naghshineh S, Barnes J, Hashemi, Y, Oldak EB (2001) United States Patent 6194366
23. Kim IK, Kang YJ, Hong YK, Park JG (2005) In: Materials Research Society symposium proceedings, pp 3–7
24. Deshpande S, Kuiry SC, Klimov M, Seal S (2005) Electrochem Solid-State Lett 8:98
25. Poling GW (1970) Corros Sci 10:359
26. Thomas D (1998) J Electrochem Soc 145:42